Progress in Natural Science: Materials International xxx (xxxx) xxx–xxx

HOSTED BY

ELSEVIER

Contents lists available at ScienceDirect

Progress in Natural Science: Materials International

journal homepage: www.elsevier.com/locate/pnsmi

Original Research

Severely deformed copper by equal channel angular pressing☆

M. Ebrahimi[a,*], C. Gode[b]

[a] Department of Mechanical Engineering, University of Maragheh, Maragheh, Iran
[b] School of Denizli Vocational Technology, Program of Machine, Pamukkale University, Denizli, Turkey

ARTICLE INFO

Keywords:
Pure copper
Equal channel angular pressing
Mechanical properties
Impact test
Microstructural observation

ABSTRACT

Mechanical and microstructural analysis of equal channel angular pressed copper was experimentally investigated. The results showed that the hardness distribution uniformity was rapidly decreased after the first pass and gradually improved at the following passes. Also, the bottom region of the pressed material experienced lower Vickers hardness magnitude irrespective of pass number. Furthermore, the addition of 0.1% magnesium to the pure copper had a considerable effect on the distribution uniformity. In addition, the material fracture mode changed from ductile to brittle by the alteration of the dimples to cleavage planes mechanism. Moreover, the formability index was dramatically reduced after the first pass and slowly improved at the succeeding passes. Eventually, ECAP process led to the increment of low angle grain boundaries and the decrease of high angle grain boundaries at the initial passes and vice versa at the subsequent ones.

1. Introduction

Demand for copper and its alloys have been vastly grown in the past two decades due to the various industrial, architectural and biological applications and also transportation and musical instruments. Its prominent merits include better mechanical properties, high electrical and thermal conductivity, acceptable corrosion resistance, suitable ductility, attractive appearance and antibacterial feature. It has been confirmed that the best circumstance of obtaining above properties is reliant on the purity condition which contains up to about 0.3% impurities even though it has low strength in comparison with the alloying situation. On the other hand, among different strength mechanisms such as solid solution, precipitation and dispersion hardenings which are based on the adding alloying elements, strain hardening seems the only way to improve the mechanical properties of pure metals without the alteration of chemical compositions [1,2].

Although there are several conventional techniques such as rolling, drawing, extrusion and forging for the enhancement of materials' strength, these mechanical improvements are usually accompanied by the sample shape change. On the other hand, recently, severe plastic deformation (SPD) method has enticed materials engineers' attention due to the imposing extremely large plastic strain without any significant changes in the sample's dimensions. This feature leads to repeat the process up to the wanted strain to obtain the desired properties [3–5]. Equal channel angular pressing (ECAP) process as one of the only few SPD techniques with the advantage of scaled up for industrial application imposes intense simple shear plastic strain through a die composing of two equal cross-sectional channels intersected at the angle of Φ with the arc of curvature, Ψ [6,7].

Up to now, there are several experimental works investigating the capability and potential of ECAP samples on the aspects of grain structure, mechanical properties, superplasticity, fatigue behavior, corrosion, wear and etc. [8–13]. The high yield and ultimate strengths, relatively low elongation to failure, the modest strain hardening value and the onset of the deformation localization at a low plastic strain have been attained at the tensile behavior of ultrafine grain (UFG) aluminum processed with the ECAP technique at the ambient temperature carried out by Ivanov and Naydenkin [14]. The study by Torre et al. [15] on the microstructure and mechanical properties of Cu samples subjected to between 1 and 16 ECAP passes indicated a transition from a microstructure dominated by lamellar boundaries to an equiaxed grain structure. Additionally, the maximum hardness, yield and ultimate tensile strengths (YS and UTS) are achieved in the fourth pass sample. From 4–16 passes, the material strength decreases and the uniform elongation increases, which have been associated to the recovery phenomenon that decreases the boundary volume and the total dislocation density. Investigation by Dobatkin et al. [16] about the influence of ECAP route and strain on the oxygen free Cu properties revealed that the strength improves by a factor of 1.6 and remains virtually constant after the fifth pass for all the routes. The maximum YS and UTS values belong to the route B_C. Furthermore, the ductility decreases after the first pass and increases after the tenth pass,

☆ Peer review under responsibility of Chinese Materials Research Society.

* Corresponding author.
E-mail address: ebrahimi@maragheh.ac.ir (M. Ebrahimi).

http://dx.doi.org/10.1016/j.pnsc.2017.03.002
Received 20 December 2016; Received in revised form 1 March 2017; Accepted 2 March 2017

especially for the route B_C. Moreover, the minimum grain size and the maximum fraction of high angle grain boundaries are respectively related to the final pass of route B_C and route A which are equal to 230 nm and 77%. A new ECAP route with a rotation angle of 60 ° (B_{60}) in the same direction between the consecutive passes was proposed and experimented by Salimyanfard et al. [17]. The results implied that the grains are more equiaxed by route B_{60} while the microstructure consists of the elongated grains in route B_C. For route B_{60}, the texture is saturated after the fourth pass, whereas the saturation in route B_C takes place after the sixth pass. In addition, the tensile strengths reach their maximum magnitudes after the eight passes during the ECAP process with both routes. Also, the fracture surface morphology of the initial and ECAP samples is similar. The temperature effect on the mechanical behavior of ECAPed copper was performed by Tao et al. [18]. The results pointed out that the flow stress of UFG Cu expresses much larger sensitivity to testing temperature than that of coarse grained (CG) one which can be related to the activation volume decrease due to the grain refinement. However, the temperature sensitivity of UFG copper to the both true strain and strain hardening rate is comparatively lower than that of CG one. The study by Zheng et al. [19] on the tensile testing of the cast Mg-Zn-Y alloy processed by ECAP method up to the eight passes at the 523 and 623 K showed the enhanced ductility in the ECAP sample with the maximum elongations of about 200% and 600%, respectively. The grain size of the as-cast alloy is also reduced from 120 μm to 3.5 μm after the final pass. The feasibility of commercial purity titanium for the dental implants after the fourth pass ECAP process at the room temperature was evaluated using cyclic bending loads by Figueiredo et al. [20]. The results indicated that despite this process improves the fatigue life as well as the yield stress and the ultimate tensile strength, the fatigue behavior of grade 1 CP Ti is slightly less satisfactory than the commercial implants fabricated by higher grade titanium alloys. Corrosion study by Mostaed et al. [21] on the multi-pass ECAP process of ZK60 Mg alloy at the different temperatures revealed, an improved corrosion resistance of the UFG alloy in comparison with the extruded one causing a shift of corrosion regime from the localized pitting at the as-received sample to a more uniform corrosion mode with the reduced localized attack at the deformed alloy. The effect of ECAP process on the wear properties of eutectic Al-12Si alloy surveyed by Kucukomeroglu [22] showed that this process decreases the wear resistance of the alloy in spite of the improvement of the strength and ductility. This phenomenon is mainly attributed to the tribochemical reaction leading to the oxidative wear with the abrasive effect in the Al-Si alloy during sliding. The oxide layer plays a dominant role in determining the wear resistance of the sample before and after the process and it masks the effect of sample strengthening on the wear resistance. The report by Nagasekhar et al. [23] stated that although strength and hardness of pure gold are increased after the ECAP process up to the four passes, following passes do not have a sizeable effect on the enhancement. In addition, the main microstructure of pressed sample is low angle grain boundaries and shear bands up to the eighth pass and equiaxed grains with high angle grain boundaries are only achieved after the twelfth pass.

By regarding the previous works, there is no complete investigation on the mechanical and microstructural properties of pure copper with and without magnesium element processed by ECAP method and in fact, this paper has been motivated by this omission.

2. Experimental material and procedure

The used pure copper for this study was in two different compositions including oxygen-free high thermal conductivity copper (Cu-OFHC) and 0.1% magnesium addition (Cu-0.1%Mg) prepared at the ER-BAKIR™ company. Accordingly, all material compositions are the same except Mg element to compare the effect of the addition of 0.1% Mg to the pure copper. The chemical composition of the Cu-OFHC material which was carried out by the spark light emission spectrometer has been listed in Table 1 in accordance with the ASTM B49 (2008) after the surface grinding for removing any oxide, oil and residues. These samples were prepared with the cylindrical shape of a 20 mm diameter and 140 mm length. Furthermore, all samples were annealed at 660 °C for 3 h which was succeeded by the furnace cooling to obtain a fully annealed material before the ECAP operation.

Table 1
Chemical composition of OFHC copper in ppm.

Cu	S	Ag	Fe	Ni	Pb	Sb
Balance	8.3	6	5	1	0.6	0.5
Cu	As	Se	Te	Cd	P	Zn
Balance	0.5	0.4	0.4	0.3	0.2	0.2
Cu	Bi	Sn	Co	Cr	Mn	Si
Balance	0.1	0.1	0.1	0.1	0.1	0.1

The ECAP process was carried out at the ambient temperature by the punch velocity of 2 mm/s and a die with the channel angle and outer corner angle of 90° and 17°, respectively. By considering the imposed equivalent plastic strain magnitude of 1.0675 for a single pass through the mentioned die, the deformation process was accomplished up to the four passes corresponding to the maximum plastic strain magnitude of 4.27 via route B_C in which the sample is consecutively rotated by 90° in the same direction and also, by use of MoS_2 as a lubricant to lessen the frictional force between the sample and the die interface [6,7]. The UFG structure of the deformed Cu samples in both Cu-OFHC and Cu-0.1%Mg conditions were then exposed to the various experimental evaluations, including hardness measurement, tensile properties, impact test and microstructure observation to obtain the capability of the UFG structure compared to their coarse grain (CG) counterparts in both circumstances.

Vickers micro-hardness (HV) measurement was performed according to ASTM E92 on the cross-section of the Cu samples before and after the ECAP process up to the four passes with the force and dwell time of 300 g and 20 s, respectively. At least, fifty measurements were carried out for each pass for evaluation of hardness distribution. In addition, tensile testing samples with the gauge length of 3 mm and cross-sectional area of 2 mm×1.5 mm were prepared via wire cutting machine with their tensile axis perpendicular to the pressing direction as can be observed in Fig. 1. The Applied standard for tensile testing was ASTM E8. All samples have been pulled up to the failure by means of the Instron universal test machine with the constant rate of cross-

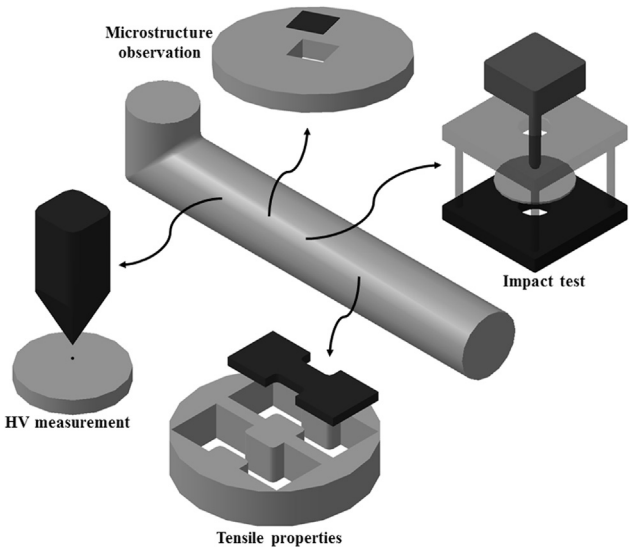

Fig. 1. Schematic representation of experimental tests on the ECAPed Cu-OFHC and Cu-0.1%Mg billets.

head displacement by the nominal strain rate of 1.0×10^{-3} s^{-1} at the ambient temperature. It should be mentioned that each test was done twice to keep away from any error. Also, scanning electron microscope (SEM) was utilized in order to investigate the fracture type of the ruptured surfaces.

Moreover, low velocity drop weight impact test was applied before and after the first and the final ECAP passes to investigate the impact behavior of the Cu samples via Instron's Dynatup 9250 HV machine in accordance with ASTM D5628. The aforementioned test was repeated three times to ensure accuracy. A tup with the definite impact energy is lifted up to a specific height and then, drops suddenly on to the sample's surface. The impact energy value which was employed by a hemisphere-shaped tup with the 12.5 mm diameter was equal to 40 J during all samples. The 3 mm thickness sample was circumferentially clamped by the pneumatic system as a fixed-fixed support. The impact loading time and velocity were respectively recorded by a load cell and a pair of photoelectric diodes and then, the magnitudes of peak load, total deflection and absorbed energy were attained and compared with each other.

Furthermore, field emission scanning electron microscopy (FE-SEM) wasutilized to investigate the grain boundary map for both the Cu-OFHC and Cu-0.1%Mg samples during the ECAP process. It is needed to note that the microstructure observation was carried out in the central region of the sample's cross-section as can be seen in Fig. 1. For this aim, mechanical grinding, polishing, electropolishing and ion etch were respectively done on the sample's surface and then, EBSD image was accomplished at an accelerating voltage of 15 kV, beam current of 10 nA and step size of 350 nm.

3. Results and discussion

3.1. Mechanical properties

The micro-HV behavior through the cross-section of both Cu-OFHC and Cu-0.1%Mg samples have been plotted in Fig. 2 before (Pass 0) and after the first and fourth passes. Referring to this figure, it can be seen that the bottom region of the ECAPed samples experiences lower plastic strain and hence, have lower HV magnitude as compared to the top zone, especially after the first pass irrespective of the material, due to the imposing of combination of the shear and bending mechanisms to the lower side. This heterogeneous behavior is gradually lessened at the subsequent passes. By considering these measurements, it can be calculated that the magnitudes of mean HV and its distribution via standard deviation (SD) factor are (43.1, 0.726), (115.3, 2.504), (135.1, 1.813) for the Cu-OFHC sample and (49.5, 0.87), (131.1, 2.22), (160.6, 1.677) for the Cu-0.1%Mg billet before and after the first and fourth passes, respectively. Accordingly, the initial condition of both materials is the most homogenous structure. Also, the HV magnitude of both samples is dramatically increased after the first pass, which indicates the enhancement of about 167% and 165% for the Cu-OFHC and Cu-0.1%Mg samples, respectively as compared to their initial states. In addition, there is a gradual improvement at the HV magnitude of the ECAPed samples at the succeeding passes. On the other hand, the first pass ECAPed samples have the maximum value of SD indicating the most heterogeneous structure and this behavior is lessened at the following passes. It can be said that approximate 255% and 150% additions at the SD value of the Cu-OFHC sample and about 155% and 93% increments at the SD value of the Cu-0.1%Mg sample are achieved after the first and fourth passes in comparison with the as-received condition. Interestingly, the subsequent passes have the profound effect on the uniformity of hardness and also, it can be noted that the copper sample with the 0.1% magnesium shows better hardness distribution uniformity as compared to the OFHC one.

Tensile testing results of the copper materials processed by the ECAP method have been represented in Table 2 including the magnitudes of YS, UTS and elongation to failure (El). As can be observed, a sharp enhancement at both yield and ultimate tensile strengths have been attained after the first pass which are equal to 117% and 122% for the Cu-OFHC and Cu-0.1%Mg samples, respectively as compared to the initial conditions. Additionally, the main reduction at the tensile ductility has been observed after the one pass ECAP process. It can be also found that further pass number has a small effect on the tensile properties. The YS and UTS magnitudes increase from 208 MPa and 311 MPa at the first pass to 331 MPa and 388 MPa at the fourth pass for the OFHC copper samples while, for the 0.1% magnesium addition to the copper samples, they reach 404 MPa and 456 MPa at the final pass from 251 MPa and 355 MPa at the first pass, respectively. Moreover, the fracture elongation corresponding to these ECAP pass numbers decreases with the gentle slope. According to the study by Goodarzy et al. [24], it can be inferred that the tensile ductility reduction of both copper samples after the ECAP process may be related to the presence of shear bands in which they can increase the intensity of planar slip trespassing on a grain boundary leading to a low energy intergranular fracture surface. On the other hand, interestingly, the strength improvement of Cu-0.1%Mg is a little more than that of Cu-OFHC which is consistent with the HV outcomes.

To evaluate material performance after the ECAP process, formability index which is defined as the multiplication of both UTS and El has been applied and the results for the various pass numbers in both copper materials have been listed in Table 3 [25]. As can be observed, imposing ECAP process leads to the reduction of formability index, while this factor is gradually increased by adding pass number. On the other hand, the highest formability index is related to the as-received situations.

SEM observation of the fractured surface after the tensile test for the different ECAP pass numbers in addition to the annealed conditions has been exhibited in Fig. 3. As can be seen in Fig. 3a, the initial condition of both Cu-OFHC and Cu-0.1%Mg materials has a large number of non-uniform dimples and micro-voids, pointing to the presence of ductile fracture type. The employment of one pass ECAP process for the both samples leads to the reduction of dimples and creating of cleavage planes, indicating the existence of mixed ductile-brittle fracture type which has been demonstrated by the tensile ductility reduction; see Fig. 3b. For the final ECAP pass number of samples, the presence of cleavage planes is intensified and the existence of dimples is decreased which is associated with the brittle fracture type according to Fig. 3c. The same behavior has been previously reported on the ECAP process on the ZK60 Mg alloy [21], Al-Cu alloy [26] and Al-Mg alloy [27].

Drop weight impact test has also been carried out on the both copper samples and the magnitudes of peak load, deflection and impact energy have been represented in Fig. 4. During this test, the force magnitude grows gradually at the loading step when the tup makes contact with the material and afterwards, it decreases rapidly at the unloading step due to the rebound. The findings indicate that ECAP process leads to the increment of peak load magnitude due to the enhancement of material strength for both copper samples. It can be said that about 6% and 13% load increments for the first and final passes have been achieved for both Cu-OFHC and Cu-0.1%Mg samples as compared to the annealed circumstances. On the other hand, deflection of ECAPed samples is decreased, which is related to the ductility reduction. For instance, there is about 25% and 48% reductions at the deflection magnitude after the first and fourth passes for the Cu-0.1%Mg sample in comparison with the initial state. Moreover, impact energy as an effecting factor to indicate material's property like the formability index has been derived. Referring to this figure, it can be said that the reduction of absorbed energy after the ECAP process is the other reason for the sample ductility diminution which has been previously demonstrated by the tensile test. Interestingly, the ECAPed Cu-0.1%Mg sample after the fourth pass has the higher impact energy as compared to the processed OFHC copper sample after the final pass. In other word, it seems that 0.1% magnesium addition to the copper

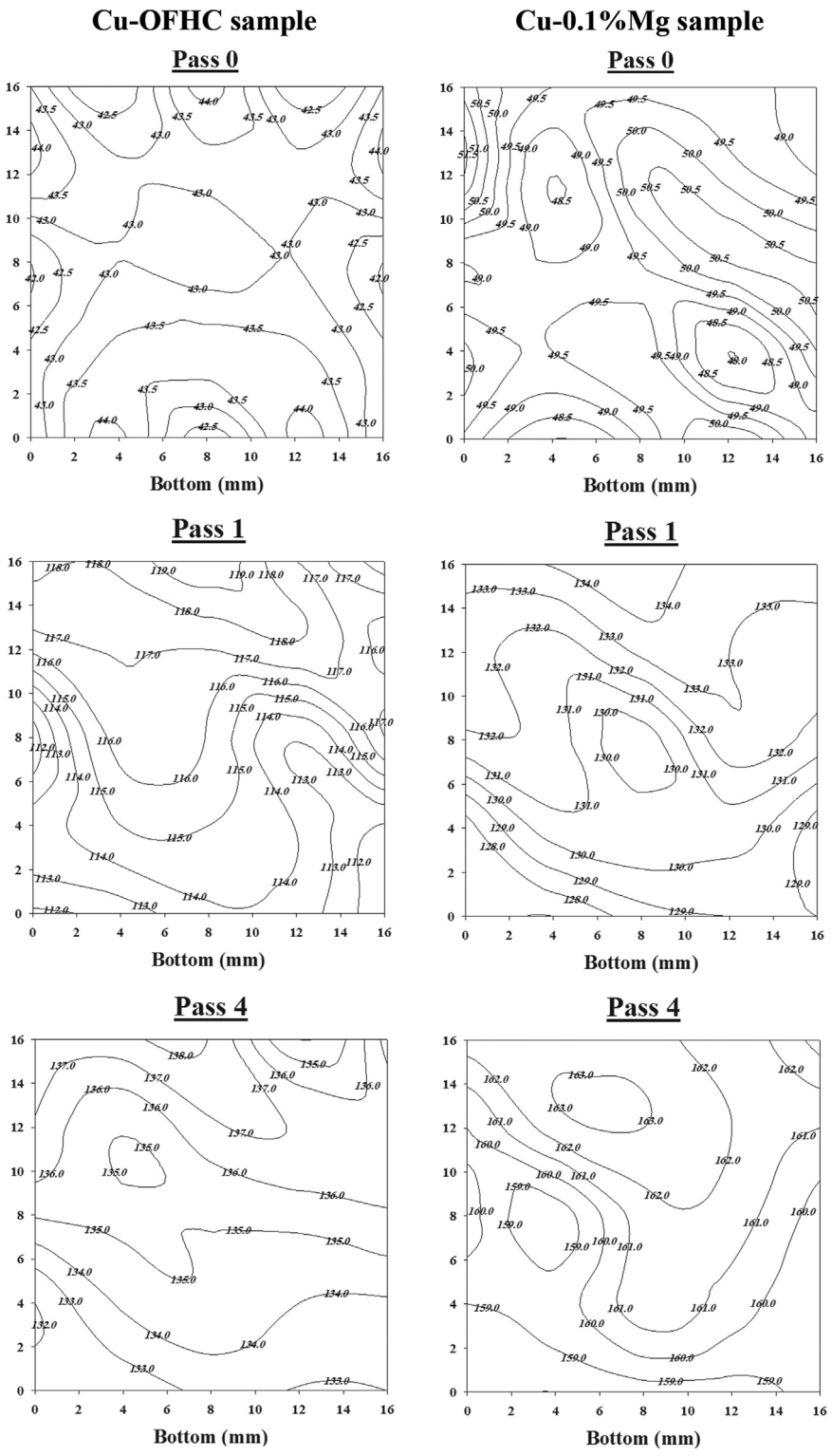

Fig. 2. Micro-HV contour map for the Cu-OFHC and Cu-0.1%Mg samples before and after the ECAP process up to the four passes.

Table 2
Magnitudes of yield strength, ultimate tensile strength and elongation to failure for the Cu-OFHC and Cu-0.1%Mg samples before and after the ECAP process up to the four passes.

	Pass 0		Pass 1		Pass 4	
	Cu-OFHC	**Cu-0.1%Mg**	**Cu-OFHC**	**Cu-0.1%Mg**	**Cu-OFHC**	**Cu-0.1%Mg**
YS (MPa)	96	113	208	251	331	404
UTS (MPa)	217	232	311	355	388	456
El (%)	37%	36%	15%	17%	14%	17%

Table 3
Formability index (MPa%) for the Cu-OFHC and Cu-0.1%Mg samples before and after the ECAP process up to the four passes.

	ECAP pass number		
Material	**Pass 0**	**Pass 1**	**Pass 4**
Cu-OFHC	80.3	46.6	54.3
Cu–0.1%Mg	83.5	60.3	77.5

billet results in higher strength and suitable ductility after the ECAP process.

3.2. Microstructure observation

Recently, some modifications have been performed on the equation of Hall – Petch by subdividing the boundaries to the low angle (LAGBs) and high angle (HAGBs) grain boundaries. By considering the prominent role of the misorientation angle on the strengthening mechanism of ECAP process, it has been suggested that the contribution of LAGBs and HAGBs has been separately taken into the account in which the effect of LAGBs and HAGBs has been respectively employed by the square root of the dislocation density accumulated in the boundaries and by the inverse average grain size (d) as can be represented in Eqs. (1–3) [28–30].

$$\sigma = \sigma_0 + \sigma_{LAGBs} + \sigma_{HAGBs} \quad (1)$$

$$\sigma_{LAGBs} = M\alpha G b \rho^{1/2} \quad (2)$$

$$\sigma_{HAGBs} = Kd^{-1/2} \quad (3)$$

Where; σ, σ_0, σ_{LAGBs} and σ_{HAGBs} denote the yield strength, flow stress of the material before the deformation and LAGBs and HAGBs strengthening contribution, respectively. Additionally, M, α, G, b and ρ are Taylor factor, crystalline constant, shear modulus, Burgers vector and total dislocation density. The grain boundary map of the two types of copper materials before and after the ECAP process achieved by EBSD analysis has been shown in Fig. 5.

Fig. 6 has been also extracted from the grain boundary map to evaluate the fraction of LAGBs and HAGBs for both the Cu-OFHC and Cu-0.1%Mg samples before and after the ECAP process up to the four passes. It is needed to say that the misorientation angle of 15° has been considered as the frontier of the low and high angle grain boundaries. It can be noted that the annealed copper materials have a large number of HAGBs with the fraction of 91% and 79% for the Cu-OFHC and Cu-0.1%Mg billets, respectively. Imposing of plastic strain with the magnitude of about 1 leads to the remarkably increment of the LAG boundaries by a factor of 6 and 3 for the copper materials without and with the Mg element. The attained boundary map reveals that the

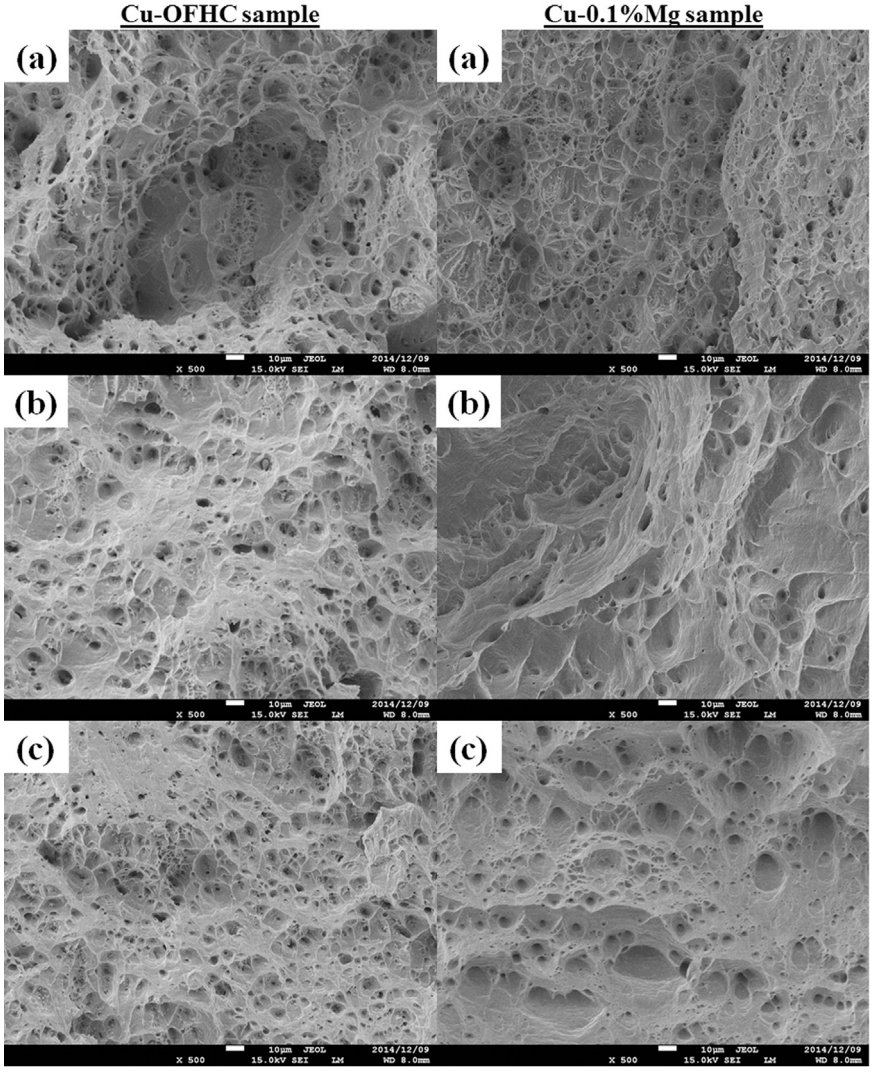

Fig. 3. Scanning electron microscope observation of the fracture surface after the tensile test for both Cu-OFHC and Cu-0.1%Mg samples (a) before and after (b) the first and (c) the final passes of ECAP process.

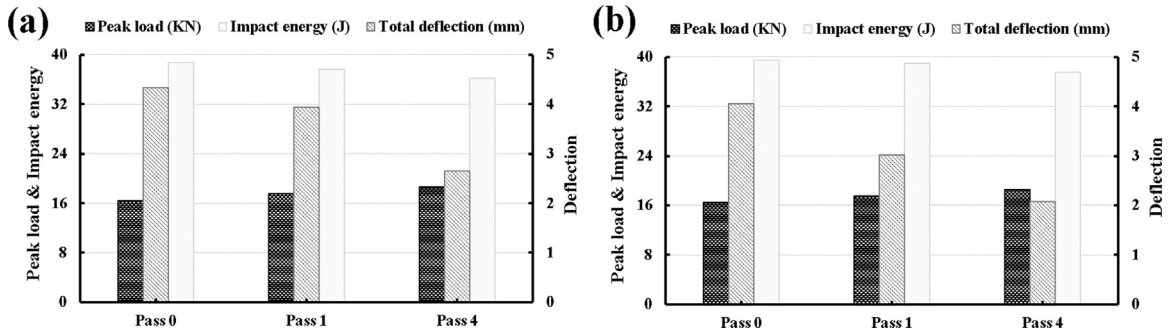

Fig. 4. Variation of peak load, total deflection and impact energy for the both (a) Cu-OFHC and (b) Cu-0.1%Mg samples before and after the first and final passes of ECAP process.

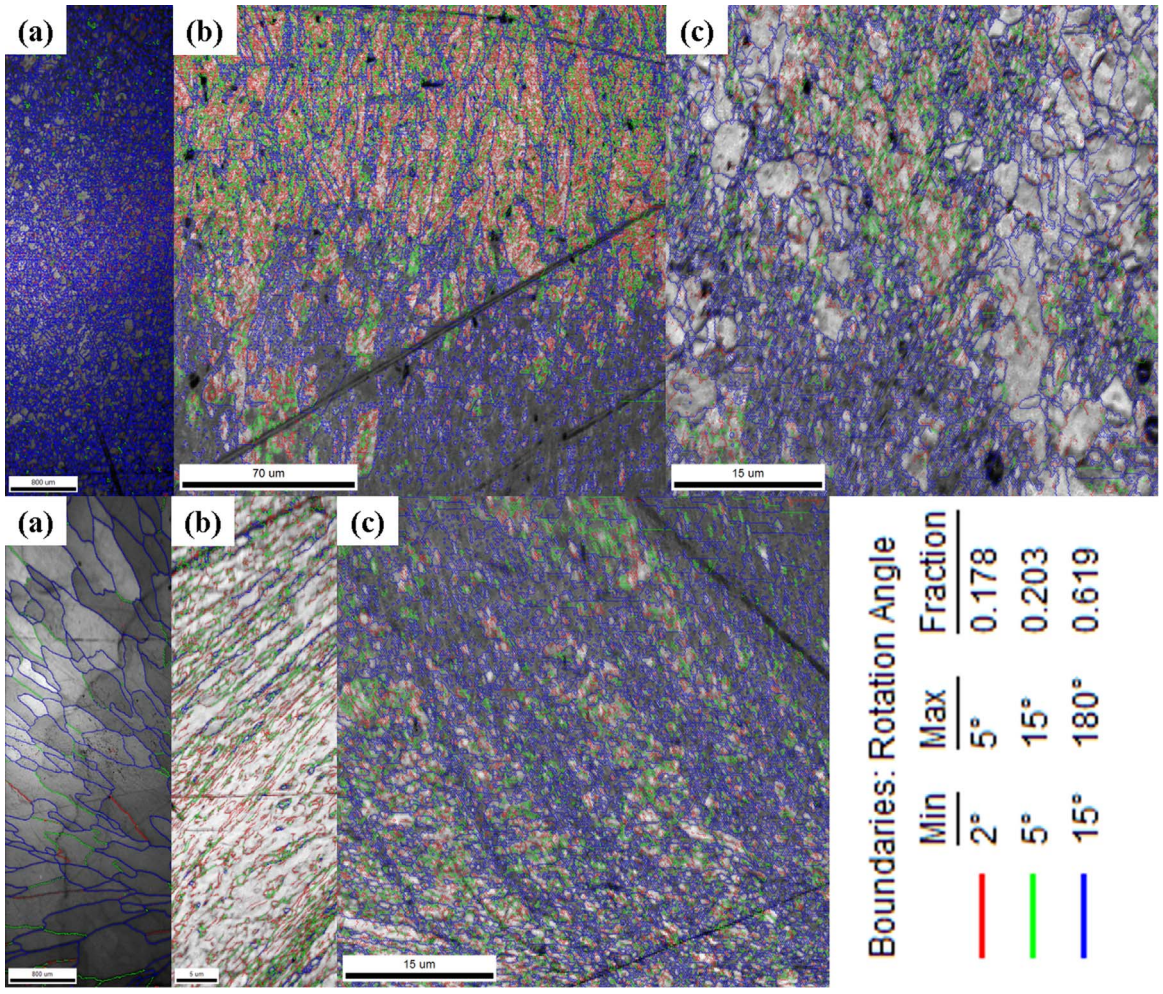

Fig. 5. Grain boundary map for both the Cu-OFHC (above) and Cu-0.1%Mg (below) samples (a) before and after (b) the first and (c) the final passes of ECAP process.

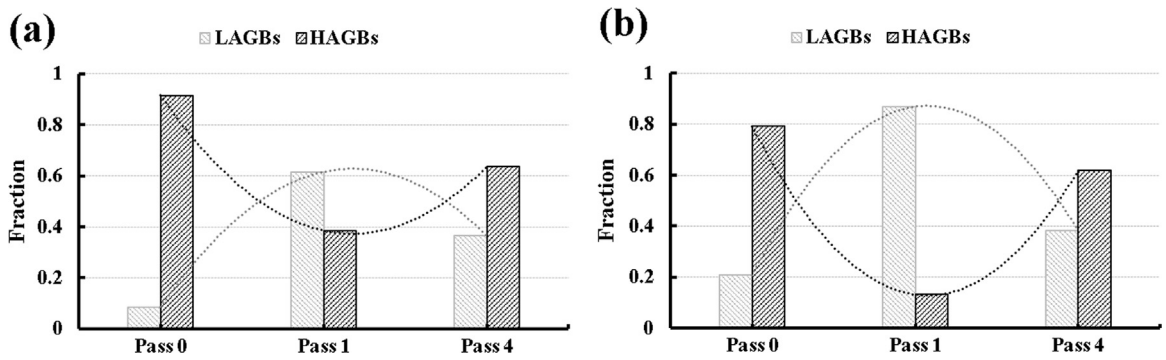

Fig. 6. Fraction of low angle grain and high angle grain boundaries for both (a) Cu-OFHC and (b) Cu-0.1%Mg samples before and after the first and final passes of ECAP process.

successive passes cause the reduction of LAGBs and increase of HAGBs in which only about 30% and 22% reductions at the HAGBs' fraction of the Cu-OFHC and Cu-0.1%Mg samples have been respectively achieved after the final pass in comparison with the annealed states. It seems that the main role of LAGBs is related to the increment of material strength while the HAGBs' influence causes mostly the homogeneity of the processed material.

4. Remark conclusions

The copper samples in two different conditions have been deformed by equal channel angular pressing process at the ambient temperature up to the four passes, and then the hardness behavior, tensile properties, fractography, drop weight impact test and structure morphology obtained and investigated. The main conclusions can be drawn as follows:

- Although the addition of 0.1% magnesium to the pure copper does not have the considerable effect on the mean HV magnitude, the hardness distribution uniformity is increased by a factor of approximately 1.6.
- Formability index as the material performance factor is dramatically decreased after the first pass and is gradually enhanced at the subsequent passes irrespective of the used chemical composition.
- Peak load and deflection which are the indicators of the material strength and ductility are respectively increased and decreased by the ECAP process.
- The boundary map examination reveals that the fraction of HAGBs changes from 0.914 and 0.792for the as-received conditions to 0.636 and 0.619 for the final pass of the Cu-OFHC and Cu-0.1%Mg samples, respectively.

Acknowledgment

This research was supported by Scientific and Technological Research Council of Turkey (**TÜBITAK**) under the 2216 Research Fellowship Program for Foreign Citizens, and the Iran Nanotechnology Initiative Council (**INIC**). The authors also would like to appear their thankfulness to the Mr. HalilGoker (Director of Er-Bakir™ Company).

References

[1] D.M. Stefanescu, ASM HANDBOOK, in: Met. Handb., 9th ed., ASM International, 1988.
[2] A.J. Ardell, Metall. Trans. A 16 (1985) 2131–2165.
[3] R.Z. Valiev, R.K. Islamgaliev, I.V. Alexandrov, 45, 2000, pp. 103–189.
[4] V.V. Popov, E.N. Popova, a.V. Stolbovskiy, Mater. Sci. Eng. A. 539 (2012) 22–29.
[5] B. Cherukuri, T.S. Nedkova, R. Srinivasan, Mater. Sci. Eng. A 410–411 (2005) 394–397.
[6] R.Z. Valiev, T.G. Langdon, Prog. Mater. Sci. 51 (2006) 881–981.
[7] F. Djavanroodi, M. Ebrahimi, Mater. Sci. Eng. A 527 (2010) 1230–1235.
[8] M.H. Shaeri, M.T. Salehi, S.H. Seyyedein, M.R. Abutalebi, J.K. Park, Mater. Des. 57 (2014) 250–257.
[9] T.G. Langdon, Mech. Mater. 67 (2013) 2–8.
[10] F. Djavanroodi, M. Ebrahimi, B. Rajabifar, S. Akramizadeh, Mater. Sci. Eng. A 528 (2010) 745–750.
[11] Z.J. Zheng, Y. Gao, Y. Gui, M. Zhu, Corros. Sci. 54 (2012) 60–67.
[12] M. Ebrahimi, S. Attarilar, F. Djavanroodi, C. Gode, H.S. Kim, Mater. Des. 63 (2014) 531–537.
[13] S.R. Kumar, K. Gudimetla, P. Venkatachalam, B. Ravisankar, K. Jayasankar, Mater. Sci. Eng. A 533 (2012) 50–54.
[14] K.V. Ivanov, E.V. Naydenkin, Mater. Sci. Eng. A 606 (2014) 313–321.
[15] F. Dalla Torre, R. Lapovok, J. Sandlin, P.F. Thomson, C.H.J. Davies, E.V. Pereloma, Acta Mater. 52 (2004) 4819–4832.
[16] S.V. Dobatkin, J.A. Szpunar, A.P. Zhilyaev, J.-Y. Cho, A.A. Kuznetsov, Mater. Sci. Eng. A 462 (2007) 132–138.
[17] F. Salimyanfard, M.R. Toroghinejad, F. Ashrafizadeh, M. Hoseini, J.A. Szpunar, Mater. Des. 44 (2013) 374–381.
[18] T. Suo, Y. Li, K. Xie, F. Zhao, K. Zhang, Y. Liu, Mater. Sci. Eng. A 527 (2010) 5766–5772.
[19] M.Y. Zheng, S.W. Xu, K. Wu, S. Kamado, Y. Kojima, Mater. Lett. 61 (2007) 4406–4408.
[20] R.B. Figueiredo, E.R. de, C. Barbosa, X. Zhao, X. Yang, X. Liu, P.R. Cetlin, T.G. Langdon, Mater. Sci. Eng. A 619 (2014) 312–318.
[21] E. Mostaed, M. Hashempour, A. Fabrizi, D. Dellasega, M. Bestetti, F. Bonollo, M. Vedani, J. Mech. Behav. Biomed. Mater. 37 (2014) 307–322.
[22] T. Kucukomeroglu, Mater. Des. 31 (2010) 782–789.
[23] G. Purcek, H. Yanar, O. Saray, I. Karaman, H.J. Maier, Wear 311 (2014) 149–158.
[24] M.H. Goodarzy, H. Arabi, M. a. Boutorabi, S.H. Seyedein, S.H. Hasani Najafabadi, J. Alloy. Compd. 585 (2014) 753–759.
[25] N. Haghdadi, a. Zarei-Hanzaki, D. Abou-Ras, Mater. Sci. Eng. A 584 (2013) 73–81.
[26] D.R. Fang, Z.F. Zhang, S.D. Wu, C.X. Huang, H. Zhang, N.Q. Zhao, J.J. Li, Mater. Sci. Eng. A 426 (2006) 305–313.
[27] D.R. Fang, Q.Q. Duan, N.Q. Zhao, J.J. Li, S.D. Wu, Z.F. Zhang, Mater. Sci. Eng. A 459 (2007) 137–144.
[28] M.M. Abramova, N. a. Enikeev, R.Z. Valiev, a. Etienne, B. Radiguet, Y. Ivanisenko, X. Sauvage, Mater. Lett. 136 (2014) 349–352.
[29] M. Reihanian, R. Ebrahimi, N. Tsuji, M.M. Moshksar, Mater. Sci. Eng. A 473 (2008) 189–194.
[30] N. Gao, M.J. Starink, M. Furukawa, Z. Horita, C. Xu, T.G. Langdon, Mater. Sci. Eng. A 410–411 (2005) 303–307.